

AUTOMATED OPTIMIZATION OF THE NON-AXISYMMETRIC HUB ENDWALL OF THE ROTOR OF AN AXIAL COMPRESSOR

Oliver Reutter, Simon Hervé, Eberhard Nicke

Department Fan and Compressor, Institute of Propulsion Technology, German Aerospace Center
DLR, Linder Hoehe, Cologne, Germany, oliver.reutter@dlr.de

ABSTRACT

In this study an axial compressor consisting of four stages is studied. The endwall of the hub of the last rotor is modified in an automated optimization process in order to reduce the losses and gain surge margin. The endwall is allowed to take non-axisymmetric shapes and is parametrized in such a way, that a groove along the suction side and a fillet are the basic forms. Additionally the lower part of the blade is allowed to vary, while the upper part remains fixed. In order to save calculation time only a set up consisting of stator 3, rotor 4 and stator 4 is calculated during the optimization process. The boundary conditions of the calculations are taken from CFD calculations of the complete four stage rig. For CFD calculations the DLR in-house TRACE-code is used. The optimization tool is AutoOpti, a DLR developed tool, which is based on a genetic algorithm speeded up by surrogate models. In the optimization two operating points are taken into account. One is the aerodynamic design point (ADP), the other one is an operating point near the surge limit (OPSL).

The basic forms which evolved during the optimization are a large fillet at the leading edge and the long stretched groove along the suction side of the blade. The optimization shows that a significant reduction of turbulent eddy viscosity and corner stall can be achieved. As the reduction of total pressure losses is limited to the hub region, thus is the overall gain in isentropic efficiency, which rises about 0.2 % in the ADP, for the OPSL an efficiency gain of about 0.5% can be reached. Especially the OPSL shows a strong reduction in secondary flow and correspondingly in corner stall. As only the hub region of the rotor is changed the overall total pressure characteristic of the stage remains basically the same. Using non-axisymmetric endwall shaping can contribute to enhancing axial stages with already highly efficient blading.

NOMENCLATURE

a	Shape factor for Gauss curves
ADP	Aerodynamic design point
CPUh	hour of usage of a 2.2 Ghz Central Processing Unit in a cluster
LE	Leading edge
OP	Operating point
OPSL	Operating point near surge limit
PS	Pressure side
R	Radius [m]
RANS	Reynolds-averaged Navier-Stokes equations
S3-R4-S4	Stator3-Rotor4-Stator4 configuration
SS	Suction side
TE	Trailing edge
TRACE	Turbomachinery research aerodynamics computational environment
η_{is}	Isentropic efficiency

INTRODUCTION

Because of the generally high level of efficiency in turbomachinery, the interest in secondary air

flows is increasing and new methods and designs are being developed to influence them and thus reduce losses, for example those induced by corner stall. In this study the geometries are based on the work of Dorfner (2009, 2011), described in the next chapter.

The objective of this study is to increase the working range and the efficiency of a 4-stage compressor, Rig 250, using an endwall contouring on the hub of the last rotor (see Fig. 1). This rotor has an optical access on the rig at DLR Cologne and thereby allows detailed measurements. Therefore it has been selected for this study. Tests with an optimized contoured endwall are planned in future. The numerical setup for this study consists of stator 3, rotor 4 and stator 4 (S3-R4-S4), where stator 3 and stator 4 have a cantilevered design. The boundary conditions are taken from calculations of the complete compressor. This study aims at improving a rotor with an already high isentropic efficiency of 94 %.

The design of the contoured endwall is realized with the help of EndwallShaping and the numerical simulation is performed by the RANS-solver TRACE, both DLR in-house tools. EndwallShaping realizes the modification of the geometry by a parametrization, and the parameters are implemented in the optimizer AutoOpti, also a DLR in-house tool.

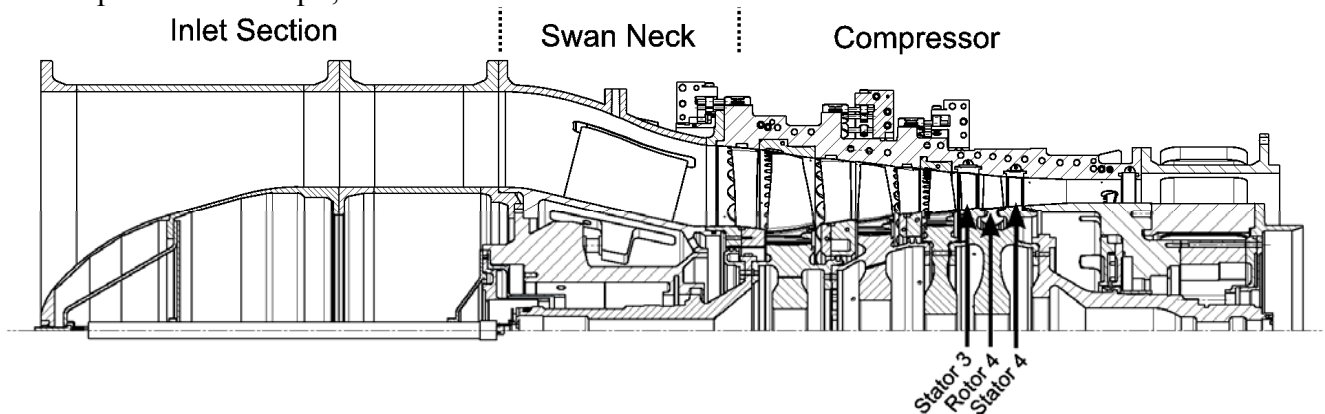


Figure 1: Rig250: Numerical Setup consisting of stator 3, rotor 4 and stator 4.

STATE OF THE ART FOR CONTOURED ENDWALLS

With the emergence of CFD and optimization tools in the past ten years, a lot of research has been conducted in the 3D-design of contoured endwalls. The new calculation capacities allow developing new complex geometries of 3D non-symmetrical contours for turbomachinery. The CFD calculations can be combined with optimization tools which modify the geometry and optimize it with respect to objective functions such as the isentropic efficiency or the total pressure ratio.

Harvey (2008) detailed the origin of the losses and the secondary flows in compressors and turbines. He gives an overview of endwall contouring in compressors as well as Gier et al. (2002).

Early works on axisymmetrical endwall contouring were realized by Spear and Biederman (1995) and a similar patent was developed by Hoeger and Schmidt-Eisenlohr (2000), illustrated by the paper Hoeger et al. (2001). These inventions developed a concave endwall which influences the position of the shock in a compressor. This new shock position reduces the losses of the stage and thus rises the efficiency. Iliopoulou et al. (2008) realized a CFD optimization of the hub of a compressor. 16 parameters were used for the parametrization of the endwall and other parameters allowed the modification of the blade. Altogether the optimization was realized with 48 parameters. An improvement of 0.4 % of the isentropic efficiency on a single rotor was achieved. The losses due to the corner stall were reduced, however the major cause of the reduction of the losses was explained to be the change of the shock position in the inlet region. Harvey (2008), Harvey and Offord (2008) showed the improvements due to contoured endwall of a single cascade and achieved a reduction of the corner stall. They stated that the influence on the pressure loss coefficient and on the exit whirl angle is similar to what can be achieved by lean and bow. In a second step, they realized a CFD-optimization on a 6-stage compressor. For this optimization, all parameters of one stage were scaled in order to parametrize the other stages, as a method to reduce the number of

parameters. In a two part paper by Reising and Schiffer (2009, a, b) an optimization of the hub and tip of a compressor based on CFD is described. An improvement of the efficiency by 1.8 % is reached with a significant reduction of the swirls on the endwall. The higher pressure gradient generated by the pseudo fillet on the suction side raises the secondary air flow but reduces the important recirculation on the suction side. The reduction of the corner stall is explained by the diminution of the static pressure on the endwall. The endwall contouring of Heinichen et al. (2011) achieved a reduction of the corner stall on a stator.

Dorfner (2009, 2011) developed a new design of endwalls. The geometry has a separation edge in front of the blade generating a swirl which counter-rotates against the secondary air flow. This swirl is guided along the blade in a groove, deflecting the secondary air flow from the suction side of the blade. Rochhausen (2010) showed the efficiency of the design developed by Dorfner on the rotor 3 of the Rig 250 also in unsteady calculations. The wake of the previous stator shortly inhibits the swirl, which reappears immediately after the passing of the wake.

During the fabrication and the milling of the blade a fillet is generated at the junction of the blade and the endwall. The influence of the fillet was shown by Kügeler et al. (2008) on a 15-stage compressor, where a simple comparison between blades with and without fillet is done. Meyer et al. (2012) realized experiments to study the influence of the size of the fillet. For the 3 fillet sizes tested (1, 3, 5 mm) the losses increase with size. Hoeger et al. (2002, 2006) realized numerical simulations to analyze the influence of a fillet and of a bulb. The bulb generates a vortex which counter-rotates against the passage vortex. In the second paper, two different fillets are tested. Globally, the fillets are beneficial in multistage compressor at the design point and part speed OPs. A very good study of the influence of the fillet is given by Müller et al. (2004), in which the leading edge of the blade in the hub region is modified. In this study a bulb form achieved the most important reduction of losses and reached about 30% at a higher incidence than design point.

METHODOLOGY

The modification of the geometry is enabled through its parametrization, described below. The blade and the endwall are parametrized separately and constructed with the DLR in-house tools BladeGenerator and EndwallShaping. The geometry is meshed with G3DHexa (Weber, 2011) having about 1 M nodes for the mesh of rotor 4 (~3 M for S3-R4-S4). It is a structured block mesh of one passage. The boundary conditions are set at the inlet and outlet of S3-R4-S4 according to calculations of the complete Rig 250. Radial equilibrium back pressure is applied, the blades have Low-Reynolds boundary conditions (y^+ values below 1.3), whereas wall functions are used at hub and shroud. The tip clearance on the rotor and the hub clearances on the stators are modeled. The geometry is calculated by TRACE, a DLR in-house CFD solver using the $k-\omega$ -model, for which recent developments are detailed in Franke et al. (2010). The convergence is checked for the global residual, the mass flow and the isentropic efficiency. The post-processing determines the performance of the geometry which has been computed by the solver.

All these steps together form the process chain which is calculated repeatedly for different geometries in an automated optimization, see Fig. 2. The optimizer, called AutoOpti, is based on an asynchronous multi-objective genetic algorithm, described further in Voss et al. (2006) and Siller et al. (2009). It generates the new members either from the current Database or from the surrogate model. The surrogate model uses the process chain without the CFD, Kriging interpolations and the expected volume gain method for finding new members, detailed in Aulich and Siller (2011). Omitting the CFD leads to a speed-up in the surrogate model from originally ~4 h per member to ~10 minutes, the Kriging trainings of the current database take about ~2 h.

Three optimizations were conducted; the first optimized only a non-symmetrical fillet (14 parameters, ~30,000 CPUh, 1028 generated members, 878 converged), the second a Dorfner-groove together with a constant fillet (13 parameters, ~22,000 CPUh, 739 generated members, 634 converged). The third optimization combined the first two with the additional freedom of varying the blade in the hub region (45 parameters, ~75,000 CPUh, 5000 generated members, 2026

converged). The design space of the third optimization includes those of the first two optimizations. For all optimizations two operating points on the 100 % speed line were evaluated, one was the aerodynamic design point (ADP) and one was close to the surge limit (OPSL). The starting/reference geometry of the first optimization had no fillet and a rotationally symmetric endwall, for the second a constant fillet from the design space of the first optimization was chosen to evaluate the additional effects of the groove. For the third optimization the starting geometry was without a fillet and with a rotationally symmetric endwall like for the first optimization. The whole blade was reconstructed with new parameters, leading to small geometric changes. This and a now needed new mesh setup led to different reference values. AutoOpti uses two independent objective functions. The objective functions for the first two optimizations were the enhancement of the isentropic efficiency of the S3-R4-S4-configuration for ADP and OPSL. For the third optimization they were changed to the reduction of the losses in the hub region (up to 20% mass flow) of the rotor for ADP and OPSL. As geometry changes were only allowed in the hub region, these last objective functions focus more on the benefits in the hub region and not on benefits obtained by flow redistribution.

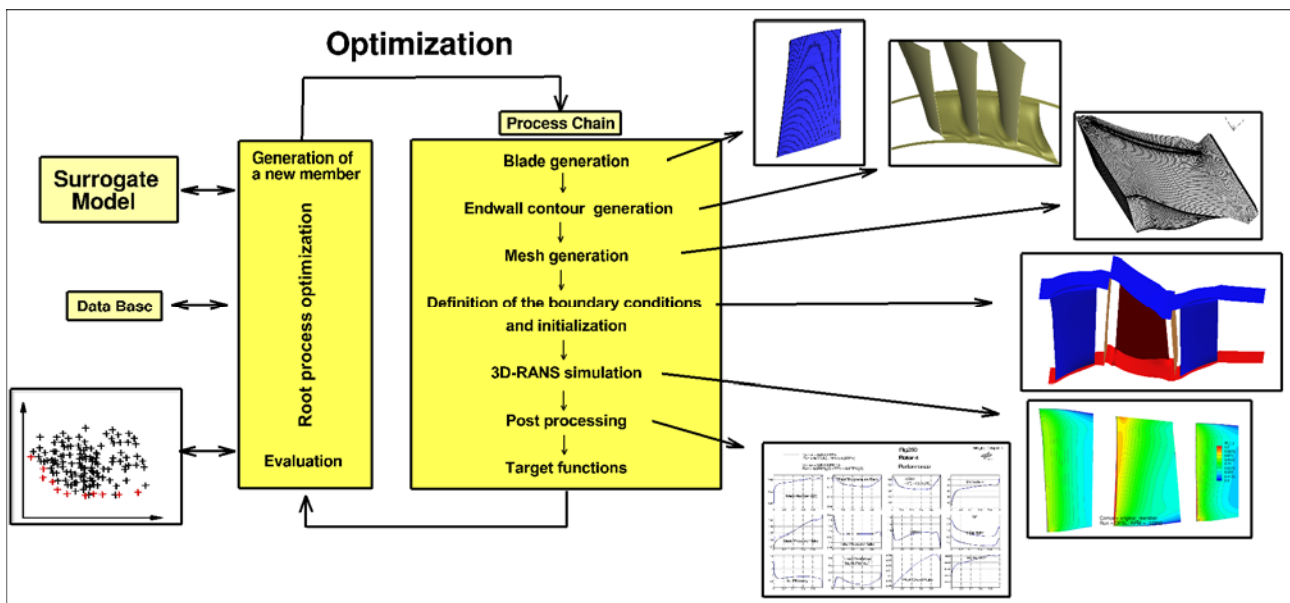


Figure 2: Process chain of the optimization.

Parametrization of the Endwall

In his work, Dorfner (2009, 2011) developed a geometry to reduce secondary air flow. The parametrization for the present study was developed with the intention of creating geometries with a fillet around the blade and a groove along the suction side having a separation edge in front of the LE. The fillet and the groove were designed and adapted by the same tool EndwallShaping.

For the description of the fillet, the parameters describe four 2D splines along the camber line: one at the LE and the TE and two splines regularly spaced in between (Fig.3). Each spline is discretized in the circumferential direction with the index i by 100 discrete points. They are defined by a Gauss curve for the radius on pressure and suction side independently, as described by the following equation:

$$R(i) = R_{PS} e^{-\left(\frac{i}{a_{PS}}\right)^2} + R_{SS} e^{-\left(\frac{i_{\max}-i}{a_{SS}}\right)^2}$$

The parameter a determines the shape of the Gauss curve. $R(i)$ is added to the rotationally symmetric contour. Depending on positive or negative $R(i)$ values material is added or taken away from this contour. At the LE and at the TE the radii are the same: $R_{SS} = R_{PS}$. For the splines I_1 and I_2 in the middle of the blade passage (Fig. 3) different radii are allowed on the two sides of the blade. Altogether, the fillet is parametrized by 14 parameters.

For the parametrization of the endwall in between the blades, the method is similar. The selected parametrization allows the construction of a separation edge and a groove. Three curves are defined and plotted in Fig. 4. The first curve is described by 4 parameters: the relative radius to create the so-called separation edge (R_{edge}), the length of the separation edge (L_{edge}), its circumferential position in the passage (Φ_{edge}) as well as its axial position (X_{edge}) between the LE of the blade and the upstream begin of the endwall; the curve is described by a Gauss curve as for the fillet and its corresponding parameters (a). For the description of the spline at the LE, 4 parameters are defined: the circumferential position of the groove (Φ_A), with the corresponding radius (R_A), and the parameters ($a1$ and $a2$) for the shape of the curve on the pressure and suction side. For the third curve the axial position (L) is defined as well as the radius (R_D) and the circumferential position (Φ_D). The parameters $a1$ and $a2$ are the same as for the spline at the LE. After the third curve, the phasing-out of the groove is interpolated linearly and a parameter (L_{end}) controls its length. 13 parameters are used to model this groove.

An example of the final geometry for a combined fillet and groove can be seen in Fig. 5. The fillet is added to the groove and both give a radial shift relative to the rotationally symmetric contour.

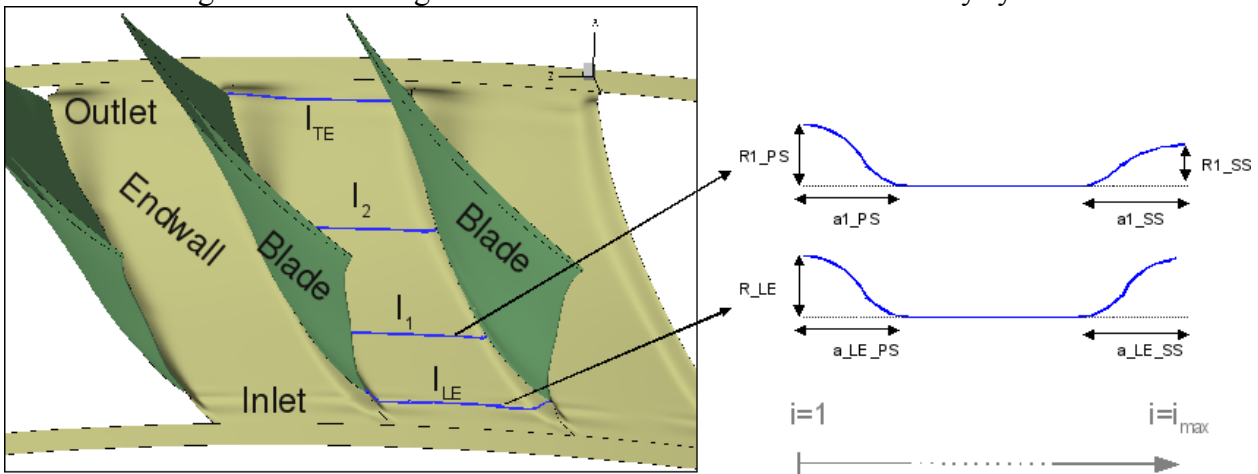


Figure 3: Parametrization of the fillet.

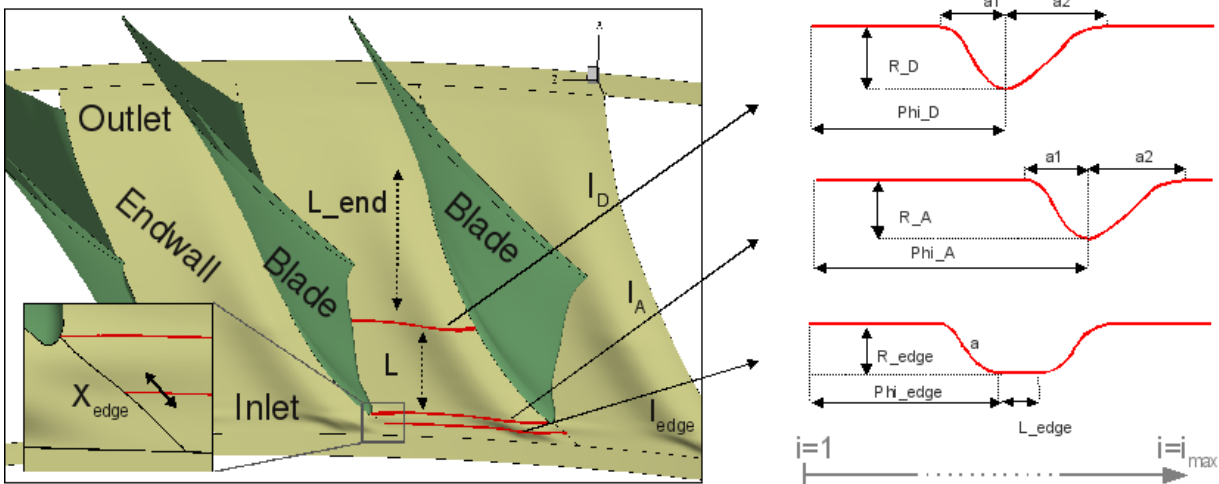


Figure 4: Parametrization of the groove.

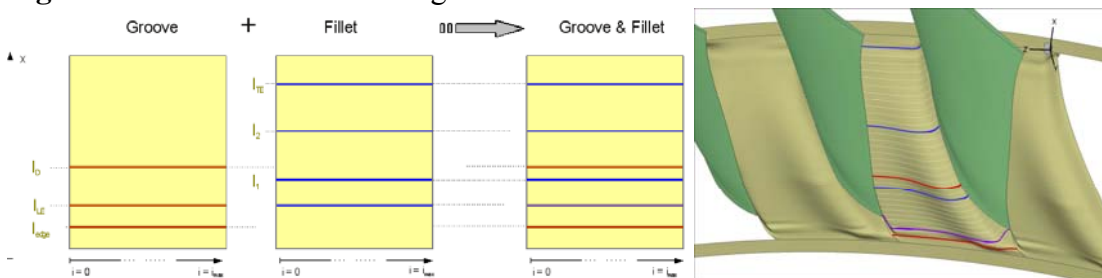


Figure 5: Addition of the relative radius of the fillet and of the groove.

Additional Parametrization of the Blade and the Meridional Contour for the Third Optimization

During the first two optimizations the rotationally symmetric base level of the meridional contour for the non-axisymmetric endwall contouring was constant. In the last optimization, two parameters are used to change it. The parameters govern the axial and the radial position of a control point, and modify the contour as can be seen on the left hand side of Fig. 6.

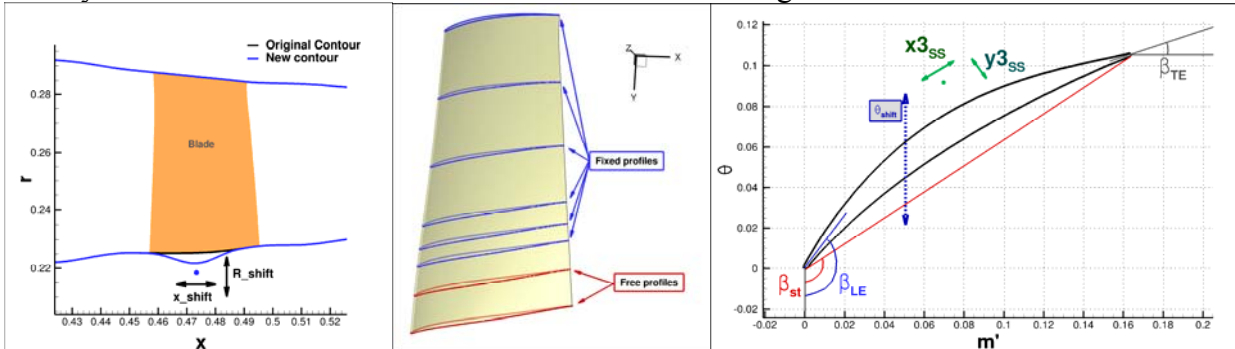


Figure 6: Parametrization of the hub endwall and the blade.

The blade is let free for optimization in the hub region up to about 20 % of the relative height. The profiles at a relative height of 18, 24, 32, 52, 76 and 100 % are fixed and ensure that only the hub region of the blade is changed.

For the two free profiles (Fig. 6, middle), the following parameters are let free: the stagger angle, the LE angle, the TE angle, the x-position and y-position of the deBoor point on the suction side and a theta shift of the whole profile in circumferential direction (Fig. 6, right). Additionally a modification of the thickness is allowed by the parametrization of the lowest profile. Four parameters control the thickness at the LE, the TE, on the pressure side and the suction side. These are 18 additional free parameters for the parametrization of the blade in the hub region, so that together with the fillet and the groove 45 parameters were used in the last optimization.

The bounds of all parameters were set very free to allow the optimization a large design space. The design of the Rig 250 does not allow the new endwall to dig more than 4 mm into the originally rotationally symmetric endwall. This was limited by the parameters, which allowed 1 cm high fillets. The steepness of the new geometry is limited by the meshing.

RESULTS

Fillet Optimization

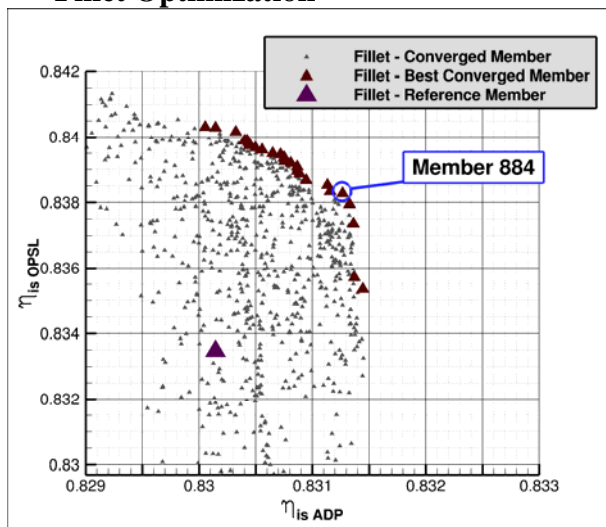


Figure 7: Pareto front of the fillet optimization

The optimization converged and a Pareto front (best members, explained in Voß 2006) developed (see Fig. 7). For all members of the Pareto front, the fillet radius at the leading edge is rather high, between 1 and 2 mm, whereas the LE radius of the profile is 0.6 mm and the maximum blade thickness 4.8 mm at the hub. The fillet radius at the trailing edge is nearly zero. A surprising effect is that there are a lot of geometries among the best members containing a negative radius for the fillet in the middle of the pressure side. This effect has also been observed by Reising and Schiffer (2009). On the suction side the fillet starts large at the leading edge, and decreases in size along the blade. It almost disappears at 3/4 of the blade length.

The size and form of the fillet at the leading edge has clearly an important influence. Big fillets are beneficial for the OPSL, and the effect is inverse for the ADP. Member 884, see Fig. 7, of the Pareto front is chosen, and the radial distribution of this member is plotted in Fig. 8. This member achieves a global improvement of 0.1 % for the ADP and of 0.4 % efficiency for the OPSL. The radial distribution shows clearly a reduction of the loss coefficient in the hub region for the OPSL, as well as a reduction of the total temperature ratio. At the ADP, the modifications on the radial distribution of the loss coefficient are very small. Furthermore, the total pressure ratio and the total temperature ratio decrease for a relative mass flow lower than 30 %.

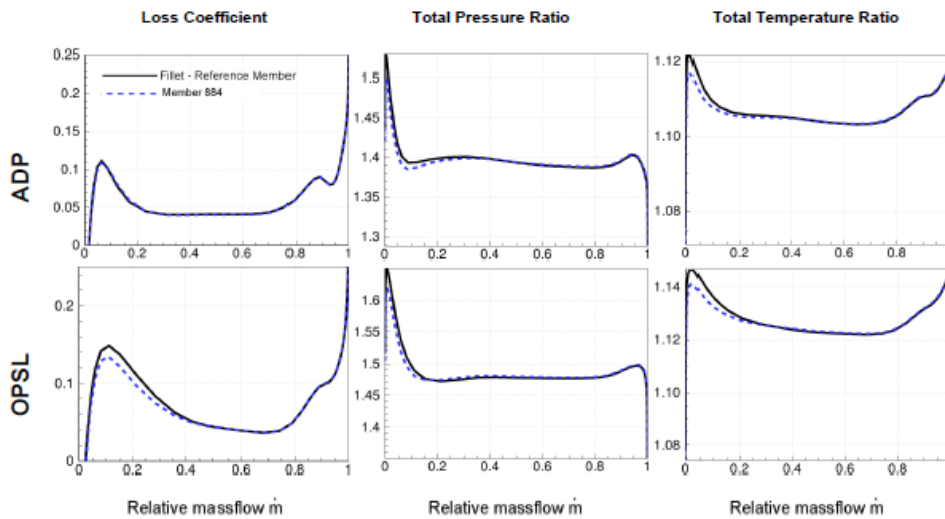


Figure 8: Radial distributions of the rotor 4 of Member 884 (see Fig. 7) of the fillet optimization.

Groove Optimization

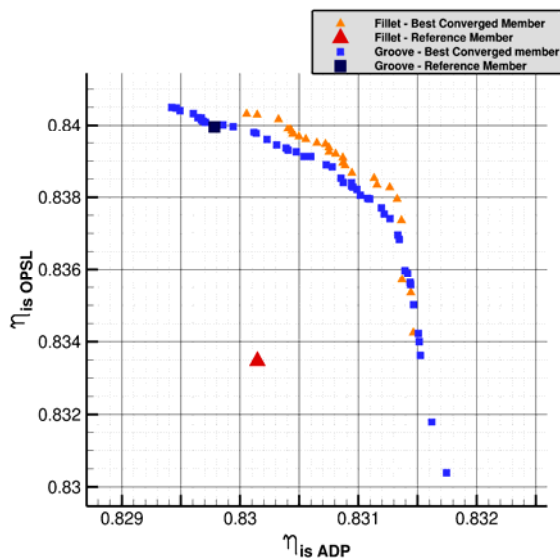


Figure 9: Pareto front of the optimization of the groove and of the fillet.

In this optimization the groove was parametrized. A fixed fillet generated by the parametrization of the endwall according to Fig. 3 with a height of about 2 mm around the blade was used in all geometries. The reference member (no groove, fixed fillet) is on the Pareto front and the members are either better in ADP or better in OPSL, see Fig. 9. This means that with this already good fillet an improvement in both operating points is not possible simultaneously, for example an increase in efficiency of 0.1 % at the ADP results in a decrease in efficiency of 0.1 % at the OPSL. The comparison with the fillet optimization shows that compared to the reference design with no fillet and no groove about the same improvements can be reached. A next optimization is necessary to use the combined potential.

The deepest groove dug about 3 mm into the rotationally symmetric reference endwall. Best at ADP were deep grooves along the suction side. Moving along the Pareto front towards those members best in OPSL moves the groove from the suction side to the pressure side and makes it shallower.

Optimization of Endwall and Blade

Restrictions are defined on the total pressure ratio in order to improve it in the optimization for both operating points, i.e. the total pressure ratio has to be greater than that of the reference for the geometry to obtain a good Pareto rank. The optimization was free to change the fillet, the groove and the hub region of the blade. The objective function was now focused on improving the losses only in the hub region. Therefore, and because of the restrictions, some members of the Pareto front shown in Fig. 10 in the same efficiency coordinate system as the previous optimizations seem to be dominated by other members. Due to the parametrization of the blade the reference member is different from the previous optimizations. It does not have a fillet, as the optimization is free to vary it. Globally, the optimization achieved a maximum improvement of the isentropic efficiency of 0.2 % for the ADP and 0.5 % for the OPSL. The improvement for the OPSL is almost the same as for the previous optimizations, but the improvement obtained for the ADP is higher.

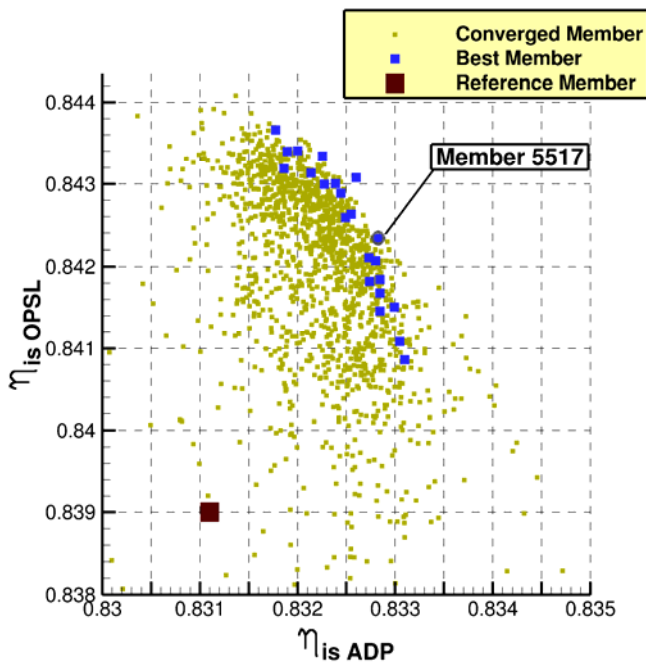


Figure 10: Pareto front of the optimization with restrictions on the total pressure ratio.

The geometries along the Pareto front all show a large fillet at the leading edge and nearly no fillet at the trailing edge. This is similar to the findings in the fillet optimization. The Pareto front members all have groove running along the suction side of the blade. In contrast to the groove optimization the groove does not change its position much along the Pareto front, but the blade, especially its LE-angle adjusts to the different incidences at ADP and OPSL.

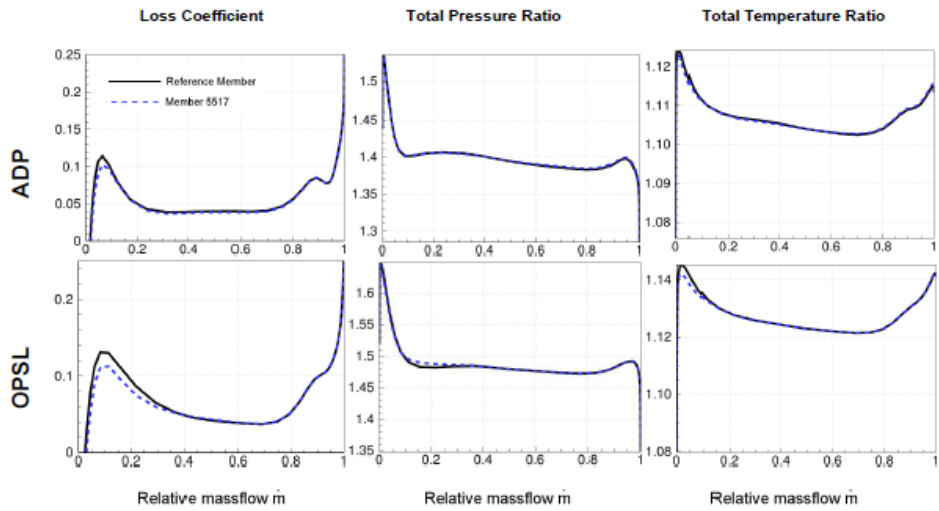


Figure 11: Radial distributions of the rotor 4 of the reference member and Member 5517.

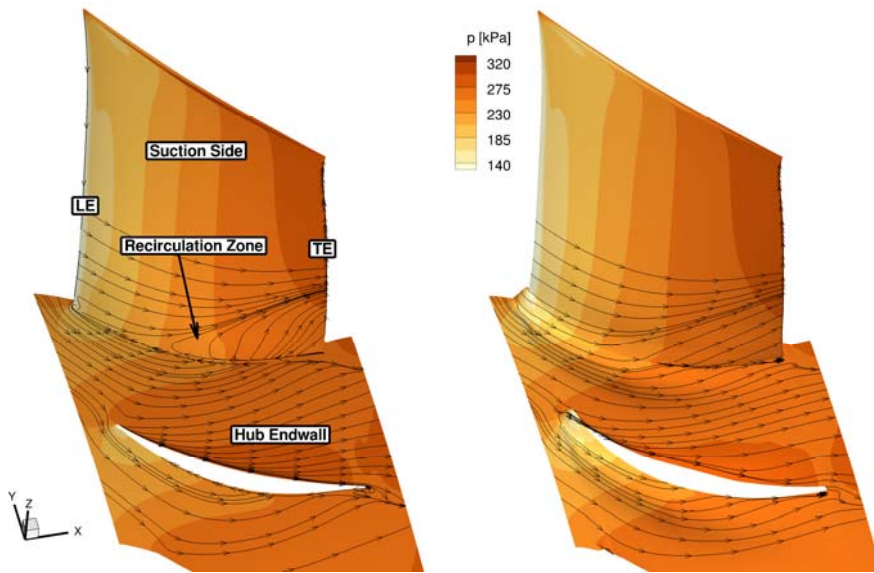


Figure 12: Improvement of the reference (left) by the Member 5517 (right) for OPSL.

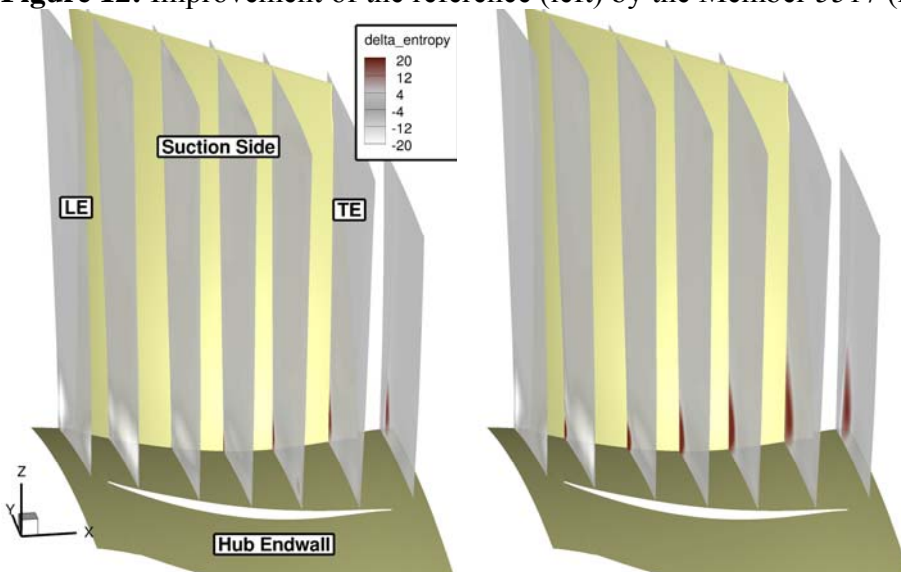


Figure 13: Delta entropy of the member 5517 compared to the reference: ADP (left), OPSL (right).

The member 5517 is further analyzed. It shows an improvement of 0.17 % in efficiency for the ADP

and of 0.33 % for the OPSL. As can be seen in Fig. 11, a significant reduction of the losses is achieved in the hub region. In Fig. 12 the streaklines show a suppression of the recirculation area on the suction side. The design is now more front-loaded, which changes the pressure distribution and reduces the pressure gradient in the passage. This can be observed in Fig. 13, where the difference in the entropy distribution between the reference member and Member 5517 is plotted for the ADP and the OPSL. The dark region corresponds to a reduction of the entropy by the optimization and an improvement of the flow. This reduction of disadvantageous flow phenomena in the corner region is observed in both operating points. The increased levels of entropy at the LE of Member 5517 can be explained by the fillet, the increase in the passage is induced by the groove, but this entropy difference disappears quickly along the chord length. The changed flow as well as the changed profile enhances the global efficiency of the blade further downstream.

CONCLUSIONS

Three optimizations allowing non axisymmetric geometry changes were conducted. First a fillet optimization showed the very high influence of the leading edge particularly for the OPSL. It demonstrated an improvement of the efficiency by 0.5 %. However the efficiency at the ADP was improved by only 0.1 %. The groove optimization showed that only one operating point can benefit from a groove. Accordingly an improvement can be obtained either for the ADP or for the OPSL. The improvement in ADP is in the order of 0.1 % with a small decrease in efficiency in the OPSL. Finally a last optimization combined the parametrization of the fillet, the groove and the blade in the hub region and the global contour. Improvements of 0.2 % for the ADP and 0.5 % for the OPSL are reached here. The improvements are now concentrated in the hub region, because the objectives (loss reduction in the hub region) focused them there.

Using non-axisymmetric endwall shaping allows new designs and can contribute to enhancing axial stages with already highly efficient blading. Further improvements need a deeper understanding of the loss mechanisms, which enables to act directly on the loss sources.

ACKNOWLEDGEMENTS

We would like to thank the DLR departments for aeronautics research and technology marketing for their support.

REFERENCES

- M. **Aulich** and U. Siller (2011), *High-dimensional constrained multiobjective optimization of a fan stage*. ASME Conf. Proc., 2011(54679):1185–1196. doi: 10.1115/GT2011-45618.
- C. **Dorfner** (2009), Entwicklung eines Verfahrens zur Konstruktion nicht-rotationssymmetrischer Seitenwandkonturen in axialen Verdichtern. PhD thesis, Univer. Bochum, ISRN DLR-FB–2009-05
- C. **Dorfner** (2011), A. Hergt, E. Nicke, and R Moenig, Advanced non-axisymmetric endwall contouring for axial compressors by generating an aerodynamic separator -part i: Principal cascade design and compressor application. *Journal of Turbomachinery*, 021026, Vol. 133, No. 2
- M. **Franke**, T. Röber, E. Kügeler, and G. Ashcroft (2010), *Turbulence treatment in steady and unsteady turbomachinery flows*, V European Conf. on CFD, Lisbon, Portugal, June 2010.
- J. **Gier**, S. Ardey, S. Eymann, U. Reinmöller, and R. Niehuis (2002), Improving 3d flow characteristics in a multistage lp turbine by means of endwall contouring and airfoil design modification – part 2: Numerical simulation and analysis, ASME GT-2002-30353, 2002.
- N. W. **Harvey** (2008), Some effects of non-axisymmetric end wall profiling on axial flow compressor aerodynamics: Part i—linear cascade investigation, ASME Conference Proceedings, 2008(43161):543–555, 2008. doi: 10.1115/GT2008-50990
- N. W. **Harvey** and T. P. Offord (2008), Some effects of non-axisymmetric end wall profiling on axial flow compressor aerodynamics: Part ii—multi-stage hpc cfd study, ASME Conference Proceedings, 2008(43161):557–569, 2008. doi: 10.1115/GT2008-50991
- F. **Heinichen**, V. Gummer, A. Plas, and H.-P. Schiffer (2011), Numerical investigation of the influence of non-axisymmetric hub contouring on the performance of a shrouded axial compressor

stator. CEAS Aeronautical Journal 13, December 2011, Volume 2, Issue 1-414, pp 89-98

M. **Hoeger** and U. Schmidt-Eisenlohr (2000), *Rotary turbomachine having a transonic compressor stage*, January 25 2000. US Patent 6,017,186

M. **Hoeger**, N. Sievers, and M. Lawrenz.(2001) *On the performance of compressor blades with contoured end walls*, In Proc. of the 4th European Conf. On Turbomach., Florence, pages 711–720

M. **Hoeger**, U. Schmidt-Eisenlohr, S. Gomez, H. Sauer, and R. Müller (2002), *Numerical simulation of the influence of a fillet and a bulb on the secondary flow in a compressor cascade*, TASK QUARTERLY, 6(1):25–37, 2002.

M. **Hoeger**, R. D. Baier, R. Müller, and M. Engber (2006), *Impact of a fillet on diffusing vane endwall flow structure*, ISROMAC 2006 - 057

V. **Iliopoulou**, I. Lepot, and P. Geuzaine (2008), *Design optimization of a hp compressor rotor blade and its hub endwall*,. ASME Conf. Proc., 2008(43161):2197–2208

E. **Kuegeler**, D. Nuernberger, A. Weber and K. Engel (2008), *Influence of blade fillets on the performance of a 15 stage gas turbine compressor*, Proc. of ASME Turbo Expo

R. **Meyer**, S. Schulz, K. Liesner, H. Passrucker, and R. Wunderer (2012), *A parameter study on the influence of fillets on the compressor cascade performance*, JTAM, 50(1):131–145

R. **Müller**, K. Vogeler, H. Sauer, and M. Hoeger (2004), *Endwall boundary layer control in compressor cascades*, ASME Turbo Expo GT2004-53433

S. **Reising** and H.P. Schiffer (2009a), *Non-axisymmetric end wall profiling in transonic compressors. part i: Improving the static pressure recovery at off-design conditions by sequential hub and shroud end wall profiling*, ASME Turbo Expo GT2009- 59133

S. **Reising** and H.P. Schiffer (2009b), *Non-axisymmetric end wall profiling in transonic compressors part ii: Design study of a transonic compressor rotor using nonaxisymmetric end walls-optimization strategies and performance*, ASME Turbo Expo GT2009-59134

S. **Rochhausen** (2010), *Untersuchung des Einflusses verschiedener Nabenkonturierungen auf das instationäre Verlustverhalten einer 1-1/2-stufigen transsonischen Verdichterkonfiguration*, Master's thesis, Technischen Universität Braunschweig

U. **Siller**, C. Voss, and E. Nicke (2009). *Automated multidisciplinary optimization of a transonic axial compressor*, AIAA Proceedings.[np]. 05-08 Jan 2009

D.A. **Spear** and B.P. Biederman (1995), *Flow directing assembly for the compression section of a rotary machine*, March 14 1995. US Patent 5,397,215.

C. **Voß**, M. Aulich, B. Kaplan, and E. Nicke (2006), *Automated multiobjective optimisation in axial compressor blade design*, ASME Conf. Proc., 2006(4241X):1289–1297

A. **Weber** (2011), *User Manual : G3D-Hexa*. DLR, 2011.